ACS APPLIED MATERIALS & INTERFACES

Research Article

www.acsami.org

Band Gap Opening in Silicene on $MgBr_2(0001)$ Induced by Li and Na

Jiajie Zhu and Udo Schwingenschlögl*

PSE Division, King Abdullah University of Science and Technology, Thuwal 23955-6900, Kingdom of Saudi Arabia

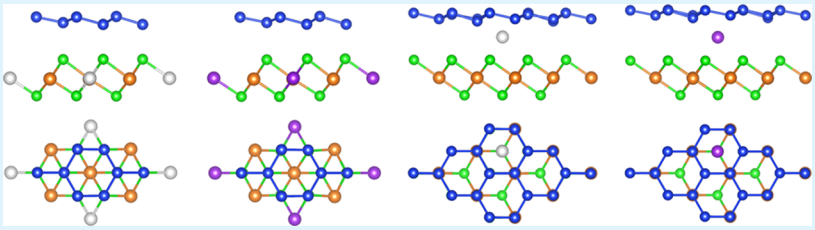

ABSTRACT: Silicene consists of a monolayer of Si atoms in a buckled honeycomb structure and is expected to be well compatible with the current Si-based technology. However, the band gap is strongly influenced by the substrate. In this context, the structural and electronic properties of silicene on $MgBr_2(0001)$ modified by Li and Na are investigated by first-principles calculations. Charge transfer from silicene (substrate) to substrate (silicene) is found for substitutional doping (intercalation). As compared to a band gap of 0.01 eV on the pristine substrate, strongly enhanced band gaps of 0.65 eV (substitutional doping) and 0.24 eV (intercalation) are achieved. The band gap increases with the dopant concentration.

KEYWORDS: *silicene, $MgBr_2$, band gap, doping, intercalation*

1. INTRODUCTION

After the graphene hype, nowadays other two-dimensional group-IV elements such as Si and Ge receive much attention.[1−3] The monolayer honeycomb structure of Si atoms, silicene, is predicted to have massless carriers at the K point of the Brillouin zone (linearly dispersing π and π^* bands)[4,5] and to be subject to buckling, unlike graphene, because of sp^2−sp^3 hybridization.[6,7] As an example of its unusual electronic properties, strong spin−orbit coupling enables silicene to host quantum spin Hall physics.[8] Clearly, the compatibility with the current Si-based technology is much better for silicene than for other group-IV materials.

Although silicene could not yet be achieved as a freestanding sheet, it has been successfully deposited on several metallic substrates, such as $ZrB_2(0001)$,[9] Ir(111),[10] and Ag(111).[11−13] However, the π bands strongly hybridize with the substrate, destroying the Dirac cone.[14,15] Semiconducting substrates including GaS nanosheets, SiC(0001), $CaF_2(111)$, and $MgBr_2(0001)$ have been explored theoretically to overcome these strong interaction characteristics. Although GaS nanosheets are predicted to preserve the linearly dispersing π bands, the large lattice mismatch of 7.5% is a major drawback.[16] A Dirac cone with a band gap of a few meV has been achieved by H passivation of the dangling bonds on top of the Si- and C-terminated SiC(0001) surfaces.[17,18] F-terminated $CaF_2(111)$ preserves the Dirac cone with a gap of 52 meV, but control of the synthesis process is problematic.[19] In previous work, we have predicted for silicene on $MgBr_2(0001)$ a Dirac cone with a 13 meV gap due to weak van der Waals interaction.[20] The in-plane lattice constant of the substrate in this case is close to that of silicene, and preparation will not be hampered by dangling bonds.

For a semiconductor used at room temperature, usually a band gap of about 0.1 eV is desirable, whereas the band gap of silicene on $MgBr_2(0001)$ is even lower than the thermal energy (25.8 meV). Although sandwich structures could slightly increase the band gap,[20] the complexity of such an arrangement limits applications. An external electric field can enhance the band gap, but hardly more than 30 meV is achievable by experimentally accessible fields.[21,22] Stacking of silicene sheets would completely destroy the Dirac cone due to the strong interlayer interaction, whereas, for graphene (weak interaction), this is an effective strategy.[23−25] In this context, we will demonstrate in the present work a band gap opening for silicene on $MgBr_2(0001)$ by substitutional doping at the Mg site with the non-isoelectronic cations Li and Na, as a consequence of the fact that the interaction with the substrate is enhanced by the extra hole. Since adsorption of alkali metals has been demonstrated to open a band gap in silicene,[26−28] we will also address the effects of intercalation, using first-principles calculations.

2. COMPUTATIONAL METHOD

Electronic structure calculations are carried out based on density functional theory and the projector augmented plane-wave method, as implemented in the Vienna Ab-initio Simulation Package.[29] The generalized gradient approximation of Perdew, Burke, and Ernzerhof is employed for the exchange-correlation potential, and the van der Waals interaction is taken into account by the DFT-D2 method.[30] Brillouin zone integrations for the 2 × 2 supercell are performed with 6 × 6 × 1 *k*-meshes in the structure optimizations and 18 × 18 × 1 *k*-meshes in the band structure calculations. The corresponding *k*-meshes for the 4 × 4 supercell are 3 × 3 × 1 and 9 × 9 × 1, respectively. In

Received: August 7, 2014
Accepted: October 16, 2014
Published: October 27, 2014

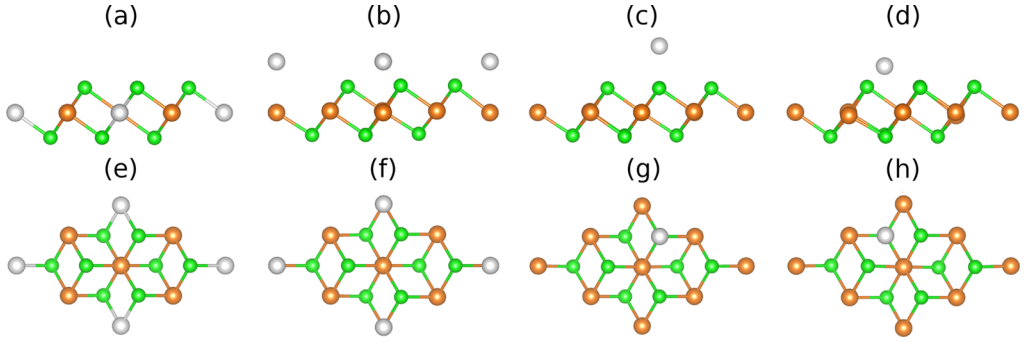

Figure 1. (a)−(d) Side views and (e)−(h) top views of $MgBr_2(0001)$ doped and decorated with Li/Na. The Mg, Br, and Li/Na atoms are brown, green, and gray.

Table 1. Structural Properties of $MgBr_2(0001)$ Decorated with Li and Na: Distance between Adatoms and Substrate ($d_{Li/Na-sub}$) and Binding Energy per Dopant Atom (E)[a]

	Li			Na		
	top Mg	top Br	top hollow	top Mg	top Br	top hollow
$d_{Li/Na-sub}$ (Å)	1.51	2.70	1.31	2.24	3.16	2.18
E (eV)	0.54	0.15	0.79	0.25	0.11	0.29

[a]The adatoms are located on top of the Mg, Br, and hollow sites.

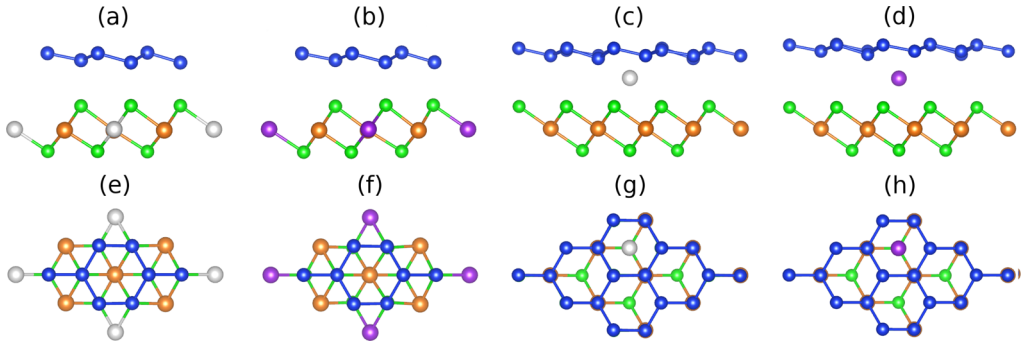

Figure 2. (a)−(d) Side views and (e)−(h) top views of silicene on $MgBr_2(0001)$ doped with Li and Na at the Mg site and intercalated on top of the hollow site. The Mg, Br, Li, Na, and Si atoms are brown, green, gray, purple, and blue.

addition, the cutoff energy for the plane-wave basis is set to 300 eV and the energy tolerance in the iterative solution of the Kohn−Sham equations to 10^{-6} eV. All structures are relaxed until the residual forces on the atoms have declined to less than 0.01 eV/Å. The calculated in-plane lattice constant of pristine $MgBr_2(0001)$ is 3.830 Å, which is in good agreement with the experimental value (3.815 Å) and close to that of freestanding silicene (3.848 Å).[31] We use 2 × 2 monolayer $MgBr_2(0001)$ as substrate and a vacuum layer of 15 Å thickness to avoid unphysical interaction between periodic images in the stacking direction. Dipole correction leads to an energy variation of less than 2 meV per atom. The dopant concentration dependence of the band gap is investigated using a 4 × 4 $MgBr_2(0001)$ supercell.

3. RESULTS AND DISCUSSION

Figure 1 shows the structure of $MgBr_2(0001)$ doped and intercalated with Li/Na at different locations, namely, at the Mg site and on top of the Mg, Br, and hollow sites. The formation energies of substitutional Li and Na doping are 1.63 and 1.92 eV in the Mg-rich limit, respectively, and −0.61 and −0.32 eV in the Br-rich limit.[32] The lower value for Li doping in the whole chemical potential range results from the smaller ionic radius (0.9, 1.16, and 0.86 Å for Li^+, Na^+, and Mg^{2+}, respectively). The bond distance to neighboring Br atoms amounts to 2.69 and 2.84 Å for Li and Na, respectively, which is a bit larger than the Mg−Br bond length (2.61 Å). The lower valence charges of Li (+0.87) and Na (+0.78) as compared to Mg (+1.61), calculated by the Bader approach, lead to weaker Coulomb interactions with the surrounding Br atoms. The structural properties obtained for Li and Na decoration are summarized in Table 1. The top of the hollow site turns out to be the most stable location because of the shortest distance to the substrate. Li sits closer to the substrate than Na due to the smaller ionic radius, since the substrate has no dangling bond.

Figure 2 illustrates the structure of silicene on $MgBr_2(0001)$ doped with Li and Na at the Mg site and intercalated on top of the hollow site. It turns out that the Si atoms prefer to be located on top of Br and the hollow site for substitutional doping and on top of Mg and Br for intercalation. Yet, both configurations are different from the case of silicene on the pristine substrate, where the Si atoms are located on top of Mg and the hollow site.[20] For substitutional doping, the interaction between the topmost Br atom and the Si atom in the lower sublattice of silicene stabilizes the system due to the Br dangling bond induced by the dopant. This results in a much larger binding energy (0.26 eV per Si atom) as compared to the pristine case (0.06 eV per Si atom). The intercalated atoms are located under the hollow site of the silicene sheet, which is the location of the topmost Br atom in the pristine case. Our results thus are in good agreement with

Table 2. Structural Properties of Silicene on $MgBr_2(0001)$ Doped with Li and Na at the Mg Site and Intercalated on Top of the Hollow Site: Si Buckling Height (b_{Si}), Distance between the Silicene Sheet and Adatom (d_{si-ad}), Distance between the Silicene Sheet and Substrate (d_{si-sub}), In-Plane Lattice Constant (a), and Binding Energy per Si Atom (E)

	Li at Mg	Na at Mg	Li on top hollow	Na on top hollow
b_{Si} (Å)	0.68	0.67	0.72	0.74
d_{si-ad} (Å)			1.35	1.61
d_{si-sub} (Å)	2.86	2.86	3.31	3.62
a (Å)	3.833	3.861	3.829	3.844
E (eV)	0.26	0.25	0.35	0.29

findings for Li and Na adsorption on freestanding silicene.[27,33,34] The unsaturated bonds again stabilize the silicene sheet, leading to a large binding energy (0.35 and 0.29 eV per Si atom for Li and Na intercalation, respectively).

The structural properties of silicene on $MgBr_2(0001)$ modified by Li and Na are listed in Table 2, showing that the lattice constants are slightly different (0.5%) from the pristine case. The Si buckling height amounts to 0.68 and 0.74 Å for substitutional doping and intercalation, respectively, which is much larger than that in freestanding silicene (0.49 Å) but still smaller than that in silicene on Ag(111) (0.75 Å).[15] Moreover, the distance between silicene and the substrate for substitutional doping (2.86 Å) is larger than that in the case of the Ag(111) substrate (2.44 Å), and the distance from the intercalated Li (1.35 Å) and Na (1.61 Å) atoms to the silicene sheet is much smaller than that in the case of freestanding silicene (1.67 and 2.19 Å, respectively).[27] The 0.65 Å upward and 0.17 Å downward shift obtained for Li and Na intercalation, respectively, leads to a larger binding energy in the former case.

Figure 3 shows charge density differences $\Delta\rho = \rho_t - \rho_{sub} - \rho_{si}$ for different systems, where ρ_t, ρ_{sub}, and ρ_{si} are the charge densities of the joint system, the substrate, and the silicene sheet, respectively. The latter two values are calculated with the same lattice paramaters and atomic positions as the joint system. We find redistribution of charge near the interface due to the interaction of the two components. For substitutional doping, a charge transfer of 0.07 electrons per Si atom from the silicene sheet to Br is found because of the Br dangling bond (which is not there in the pristine substrate). Charge redistribution also occurs within the silicene sheet from the lower sublattice to the upper sublattice. For intercalation, charge mainly transfers between the adatoms and the silicene sheet (0.09 electrons per Si atom).

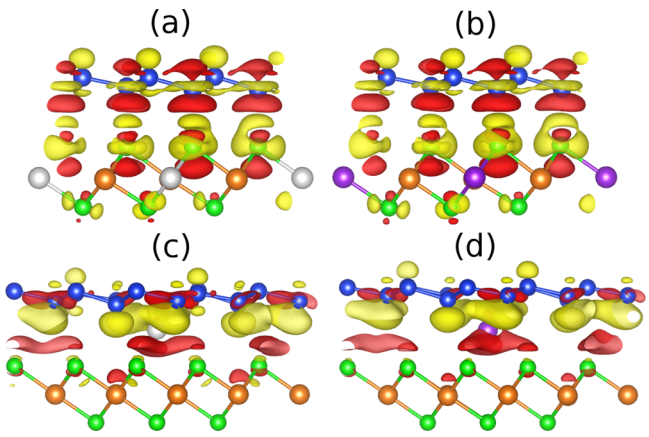

Figure 3. Charge density difference for silicene on $MgBr_2(0001)$ doped with (a) Li and (b) Na at the Mg site and intercalated with (c) Li and (d) Na on top of the hollow site. Yellow (red) color represents charge accumulation (depletion), where the isosurfaces refer to isovalues of 1.2 × 10^{-3} electrons/bohr^3. The Mg, Br, Li, Na, and Si atoms are brown, green, gray, purple, and blue.

The density of states of $MgBr_2(0001)$ doped with Li and Na at the Mg site and intercalated on top of the hollow site, without and with silicene, is addressed in Figure 4. Without silicene, the valence band maximum is composed of Br 4p states for both substitution and intercalation, whereas the conduction band minimum consists of Mg 3s states for substitution and Li/Na s and Mg 3s states for intercalation. On the other hand, when silicene is attached, it is dominated by Si 3p and Br 4p states for substitution and by Si 3p states only for intercalation. The conduction band minimum mainly consists of Si 3p states for substitution and Si 3p and Li/Na s states for intercalation. Larger hybridization between the Si 3p and Br 4p states for substitution than between the Si 3p and Li/Na s states for intercalation reflects stronger interaction.

According to the band structures shown in Figure 5, the band gap for substitutional doping turns out to be 0.65 eV at the K and K′ points of the Brillouin zone, which is much larger than that for the pristine substrate (0.01 eV). The electric field at the interface that is induced by the charge transfer breaks the symmetry of the two silicene sublattices and opens the band gap. The enhanced value is important to overcome the thermal fluctuations at room temperature, improving the applicability of the material. In addition, the Dirac point is located 0.78 eV above the Fermi level due to charge transfer to the substrate, reflecting p-type doping (Table 3). On the other hand, band gaps of only 0.24 and 0.17 eV are found for Li and Na intercalation, respectively, due to the weaker interaction. A larger gap for Li than for Na decoration due to the shorter distance to the silicene sheet also has been predicted in the case of freestanding silicene.[34] The Dirac point is located 0.58 eV (Li) and 0.56 eV (Na) below the Fermi level, which reflects charge accumulation on the silicene sheet and thus n-type doping.

We next study the dopant concentration dependence of the band gap. Different locations of the dopant atoms ranging from clusters to a homogeneous distribution are compared for each concentration, and the location of the Si atoms is tested for each case. The locations are energetically almost degenerate. According to Figure 6, the band gap increases with the dopant concentration up to 0.6 eV at 25% for substitutional doping. The abrupt change at 18.75% is due to a shift of the Si location from on top of Mg to on top of Br. The stronger Si−Br interaction stabilizes the system and opens the band gap.[20] On the other hand, the band gap increases almost linearly for intercalation, while the Si location shifts from top of the hollow site to top of Br at 25% and 18.75% for Li and Na intercalation, repectively, because of the different distances to the silicene sheet (Table 2). The band gap for Li intercalation is larger than that for Na intercalation due to the stronger interaction with the silicene sheet.

4. CONCLUSIONS

The structural and electronic properties of silicene on $MgBr_2(0001)$ modified by Li and Na have been investigated using first-principles calculations. Silicene is found to be much more stable on the modified substrate than on pristine $MgBr_2(0001)$ due to strong Si−Br interaction for substitutional doping and strong Si−Li/Na interaction for intercalation.

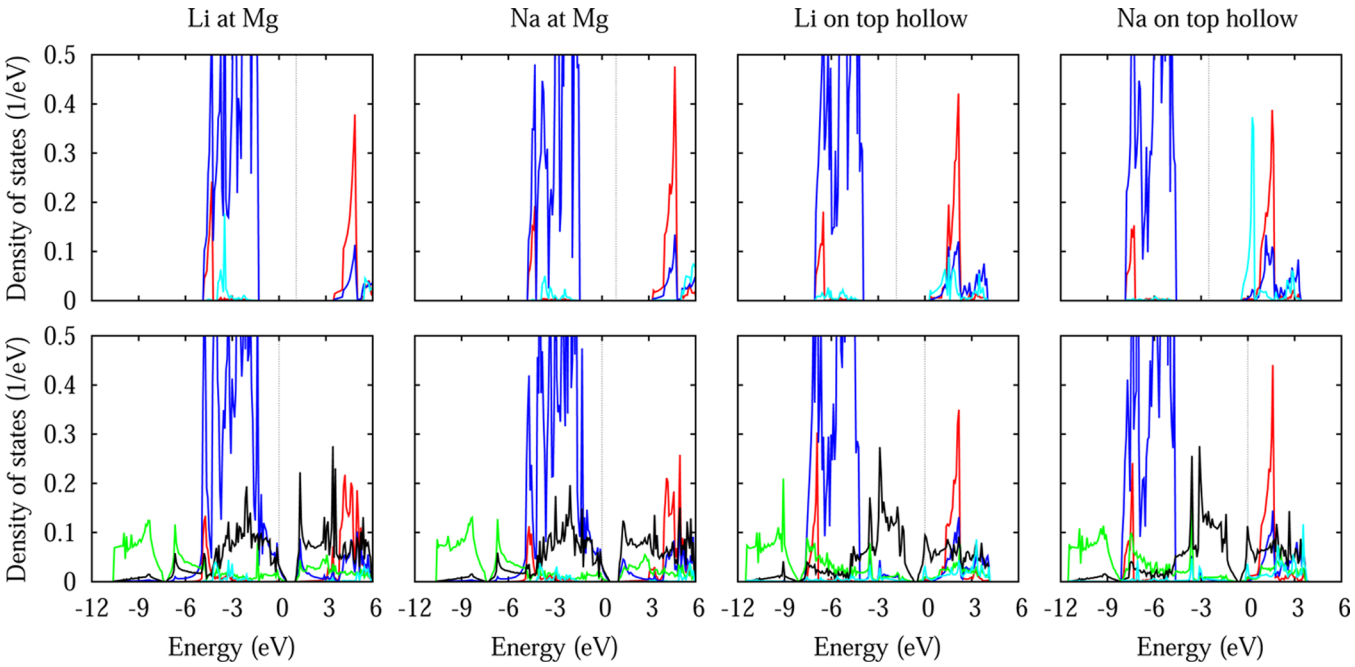

Figure 4. Density of states of $MgBr_2(0001)$ doped with Li and Na at the Mg site and intercalated on top of the hollow site, without (upper row) and with (lower row) silicene. The Fermi level is set to zero for the systems including silicene. The Mg 3s, Br 4p, Si 3s, Si 3p, and Li/Na s states are shown in red, blue, green, black, and cyan.

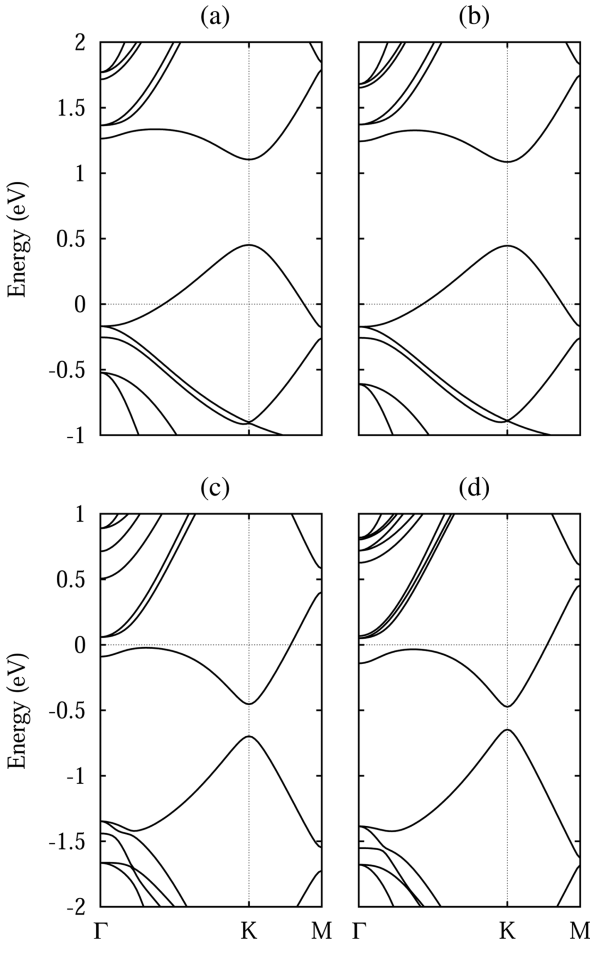

Figure 5. Band structure of silicene on $MgBr_2(0001)$ doped with (a) Li and (b) Na at the Mg site and intercalated with (c) Li and (d) Na on top of the hollow site. The Fermi level is set to zero.

Table 3. Position of the Dirac Point with Respect to the Fermi level (E_D) and Band Gap at the Dirac Point (E_g) for Different Modifications

	Li at Mg	Na at Mg	Li on top hollow	Na on top hollow
E_D (eV)	0.78	0.77	−0.58	−0.56
E_g (eV)	0.65	0.64	0.24	0.17

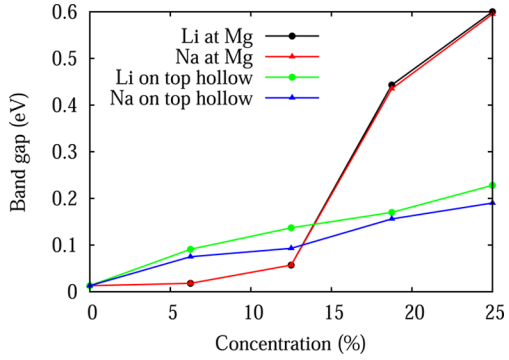

Figure 6. Concentration dependence of the band gap of silicene on $MgBr_2(0001)$ for different modifications.

Importantly, the band gap amounts to 0.65 eV, with a strong p-type character, for substitutional doping (0.01 eV on the pristine substrate) due to charge transfer to the substrate. On the other hand, a band gap of 0.24 eV (0.17 eV), with a strong n-type character, is achieved for Li (Na) intercalation due to charge transfer to the silicene sheet. Furthermore, we have demonstrated that the band gap can be flexibly tuned by means of the concentration of the dopant atoms. The enlarged band gaps induced by Li and Na are strongly desirable from the application point of view.

dx.doi.org/10.1021/am5052697 | ACS Appl. Mater. Interfaces 2014, 6, 19242−19246

AUTHOR INFORMATION

Corresponding Author

*E-mail: udo.schwingenschlogl@kaust.edu.sa (U.S.).

Notes

The authors declare no competing financial interest.

ACKNOWLEDGMENTS

Research reported in this publication was supported by the King Abdullah University of Science and Technology (KAUST).

REFERENCES

(1) Novoselov, K. S.; Geim, A. K.; Morozov, S. V.; Jiang, D.; Zhang, Y.; Dubonos, S. V.; Grigorieva, I. V.; Firsov, A. A. Electric Field Effect in Atomically Thin Carbon Films. *Science* **2004**, *306*, 666−669.

(2) Castro Neto, A. H.; Guinea, F.; Peres, N. M. R.; Novoselov, K. S.; Geim, A. K. The Electronic Properties of Graphene. *Rev. Mod. Phys.* **2009**, *81*, 109−162.

(3) Novoselov, K. S.; Fal'ko, V. I.; Colombo, L.; Gellert, P. R.; Schwab, M. G.; Kim, K. A Roadmap for Graphene. *Nature* **2012**, *490*, 192−200.

(4) Takeda, K.; Shiraishi, K. Theoretical Possibility of Stage Corrugation in Si and Ge Analogs of Graphite. *Phys. Rev. B* **1994**, *50*, 14916−14922.

(5) Cahangirov, S.; Topsakal, M.; Aktürk, E.; Şahin, H.; Ciraci, S. Two- and One-Dimensional Honeycomb Structures of Silicon and Germanium. *Phys. Rev. Lett.* **2009**, *102*, 236804.

(6) Durgun, E.; Tongay, S.; Ciraci, S. Silicon and III-V Compound Nanotubes: Structural and Electronic Properties. *Phys. Rev. B* **2005**, *72*, 075420.

(7) Roome, N. J.; Carey, J. D. Beyond Graphene: Stable Elemental Monolayers of Silicene and Germanene. *ACS Appl. Mater. Interfaces* **2014**, *6*, 7743−7750.

(8) Liu, C.; Feng, W.; Yao, Y. Quantum Spin Hall Effect in Silicene and Two-Dimensional Germanium. *Phys. Rev. Lett.* **2011**, *107*, 076802.

(9) Fleurence, A.; Friedlein, R.; Ozaki, T.; Kawai, H.; Wang, Y.; Yamada-Takamura, Y. Experimental Evidence for Epitaxial Silicene on Diboride Thin Films. *Phys. Rev. Lett.* **2012**, *108*, 245501.

(10) Meng, L.; Wang, Y.; Zhang, L.; Du, S.; Wu, R.; Li, L.; Zhang, Y.; Li, G.; Zhou, H.; Hofer, W. A.; Gao, H. Buckled Silicene Formation on Ir(111). *Nano Lett.* **2013**, *13*, 685−690.

(11) Tsoutsou, D.; Xenogiannopoulou, E.; Golias, E.; Tsipas, P.; Dimoulas, A. Evidence for Hybrid Surface Metallic Band in (4 × 4) Silicene on Ag(111). *Appl. Phys. Lett.* **2013**, *103*, 231604.

(12) Vogt, P.; De Padova, P.; Quaresima, C.; Avila, J.; Frantzeskakis, E.; Asensio, M. C.; Resta, A.; Ealet, B.; Le Lay, G. Silicene: Compelling Experimental Evidence for Graphenelike Two-Dimensional Silicon. *Phys. Rev. Lett.* **2012**, *108*, 155501.

(13) Kaltsas, D.; Tsetseris, L.; Dimoulas, A. Structural Evolution of Single-Layer Films during Deposition of Silicon on Silver: A First-Principles Study. *J. Phys.: Condens. Matter* **2012**, *24*, 442001.

(14) Lin, C.-L.; Arafune, R.; Kawahara, K.; Kanno, M.; Tsukahara, N.; Minamitani, E.; Kim, Y.; Kawai, M.; Takagi, N. Substrate-Induced Symmetry Breaking in Silicene. *Phys. Rev. Lett.* **2013**, *110*, 076801.

(15) Wang, Y.; Cheng, H. Absence of a Dirac Cone in Silicene on Ag(111): First-Principles Density Functional Calculations with a Modified Effective Band Structure Technique. *Phys. Rev. B* **2013**, *87*, 245430.

(16) Ding, Y.; Wang, Y. Electronic Structures of Silicene/GaS Heterosheets. *Appl. Phys. Lett.* **2013**, *103*, 043114.

(17) Gao, N.; Li, J.; Jiang, Q. Bandgap Opening in Silicene: Effect of Substrates. *Chem. Phys. Lett.* **2014**, *592*, 222−226.

(18) Liu, H.; Gao, J.; Zhao, J. Silicene on Substrates: A Way to Preserve or Tune Its Electronic Properties. *J. Phys. Chem. C* **2013**, *117*, 10353−10359.

(19) Kokott, S.; Pflugradt, P.; Matthes, L.; Bechstedt, F. Nonmetallic Substrates for Growth of Silicene: An ab Initio Prediction. *J. Phys.: Condens. Matter* **2014**, *26*, 185002.

(20) Zhu, J.; Schwingenschlögl, U. Structural and Electronic Properties of Silicene on MgX_2 (X = Cl, Br, and I). *ACS Appl. Mater. Interfaces* **2014**, *6*, 11675−11681.

(21) Ye, M.; Quhe, R.; Zheng, J.; Ni, Z.; Wang, Y.; Yuan, Y.; Tse, G.; Shi, J.; Gao, Z.; Lu, J. Tunable Band Gap in Germanene by Surface Adsorption. *Physica E* **2014**, *59*, 60−65.

(22) Ni, Z.; Liu, Q.; Tang, K.; Zheng, J.; Zhou, J.; Qin, R.; Gao, Z.; Yu, D.; Lu, J. Tunable Bandgap in Silicene and Germanene. *Nano Lett.* **2012**, *12*, 113−118.

(23) Liu, Y.; Shu, H.; Liang, P.; Cao, D.; Chen, X.; Lu, W. Structural, Electronic, and Optical Properties of Hydrogenated Few-Layer Silicene: Size and Stacking Effects. *J. Appl. Phys.* **2013**, *114*, 094308.

(24) Zhong, X.; Yap, Y. K.; Pandey, R.; Karna, S. P. First-Principles Study of Strain-Induced Modulation of Energy Gaps of Graphene/BN and BN Bilayers. *Phys. Rev. B* **2011**, *83*, 193403.

(25) Sławińska, J.; Zasada, I.; Klusek, Z. Energy Gap Tuning in Graphene on Hexagonal Boron Nitride Bilayer System. *Phys. Rev. B* **2010**, *81*, 155433.

(26) Ni, Z.; Zhong, H.; Jiang, X.; Quhe, R.; Luo, G.; Wang, Y.; Ye, M.; Yang, J.; Shi, J.; Lu, J. Tunable Band Gap and Doping Type in Silicene by Surface Adsorption: Towards Tunneling Transistors. *Nanoscale* **2014**, *6*, 7609−7618.

(27) Sahin, H.; Peeters, F. M. Adsorption of Alkali, Alkaline-Earth, and 3*d* Transition Metal Atoms on Silicene. *Phys. Rev. B* **2013**, *87*, 085423.

(28) Quhe, R.; Yuan, Y.; Zheng, J.; Wang, Y.; Ni, Z.; Shi, J.; Yu, D.; Yang, J.; Lu, J. Does the Dirac Cone Exist in Silicene on Metal Substrates? *Sci. Rep.* **2014**, *4*, 5476.

(29) Kresse, G.; Joubert, D. From Ultrasoft Pseudopotentials to the Projector Augmented-Wave Method. *Phys. Rev. B* **1999**, *59*, 1758−1775.

(30) Grimme, S. Semiempirical GGA-type Density Functional Constructed with a Long-Range Dispersion Correction. *J. Comput. Chem.* **2006**, *27*, 1787−1799.

(31) Pies, W.; Weiss, A. In *Key Elements: F, Cl, Br, I*; Hellwege, K.-H., Hellwege, A., Eds.; Landolt-Börnstein - Group III Condensed Matter; Springer: Berlin, 1973; Vol. *7a*; pp 520−529.

(32) Dolui, K.; Rungger, I.; Das Pemmaraju, C.; Sanvito, S. Possible Doping Strategies for MoS_2 Monolayers: An Ab Initio Study. *Phys. Rev. B* **2013**, *88*, 075420.

(33) Setiadi, J.; Arnold, M. D.; Ford, M. J. Li-Ion Adsorption and Diffusion on Two-Dimensional Silicon with Defects: A First Principles Study. *ACS Appl. Mater. Interfaces* **2013**, *5*, 10690−10695.

(34) Quhe, R.; Fei, R.; Liu, Q.; Zheng, J.; Li, H.; Xu, C.; Ni, Z.; Wang, Y.; Yu, D.; Gao, Z.; Lu, J. Tunable and Sizable Band Gap in Silicene by Surface Adsorption. *Sci. Rep.* **2012**, *2*, 853.